NATIONAL ADVISORY COMMITTEE FOR AERONAUTICS

TECHNICAL NOTE

No. 1042

PERFORMANCE TESTS OF WIRE STRAIN GAGES

IV - AXIAL AND TRANSVERSE SENSITIVITIES

By William R. Campbell
National Bureau of Standards

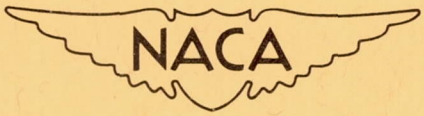

Washington
June 1946

E R R A T A

NACA TN No. 1042

PERFORMANCE TESTS OF WIRE STRAIN GAGES
IV -- AXIAL AND TRANSVERSE SENSITIVITIES
By William R. Campbell
June 1946

Table III page 20: Second column from left under Wire Alloy -- second entry

Chromel C

(0.005 in.) should be (0.001 in.)

Isoelastic

(0.005 in.) should be (0.0008 in.)

NATIONAL ADVISORY COMMITTEE FOR AERONAUTICS

TECHNICAL NOTE No. 1042

PERFORMANCE TESTS OF WIRE STRAIN GAGES

IV – AXIAL AND TRANSVERSE SENSITIVITIES

By William R. Campbell

SUMMARY

Results of calibrations to determine axial and transverse strain sensitivities are presented for 15 types of single-element, multistrand wire strain gages.

Average ratios of transverse sensitivity, K_t, to axial sensitivity, K_a, were found to be positive for 11 types of gages and K_t/K_a did not exceed 0.028 for these gages. Negative values of the average ratio K_t/K_a ranging from −0.007 to −0.063 were found for four types of gages. The negative transverse sensitivity of one type of gage was ascribed to the geometry of the gage structure. Negative transverse sensitivities for the remaining three gages were ascribed to the wire itself. The wires in these gages were characterized by having a negative transverse sensitivity coupled with a relatively high axial strain sensitivity.

INTRODUCTION

This report describes one of a series of performance tests on wire strain gages of types currently used in large numbers to measure stresses in aircraft structures. The purpose of the tests is to make available information on the properties, accuracy, and limitations of various multistrand, single-element gages.

The performance test program has been divided into several phases the results of which are being reported individually. The first three phases of the program have

been reported in references 1 to 3. The present paper reports on the fourth phase, determinations of axial and transverse gage sensitivities.

This investigation, conducted at the National Bureau of Standards, was sponsored by and conducted with the financial assistance of the National Advisory Committee for Aeronautics.

The author desires to acknowledge the cooperation of the NACA Ames Aeronautical Laboratory, the Baldwin Locomotive Works, the Boeing Aircraft Company, the Chrysler Corporation, the Consolidated Vultee Aircraft Corporation, the Douglas Aircraft Company, the Lockheed Aircraft Corporation, North American Aviation Incorporated, and Northrop Aircraft Incorporated in submitting test gages. The author is grateful for the assistance of members of the Engineering Mechanics Section of the National Bureau of Standards, and is particularly indebted to Dr. Walter Ramberg for suggesting the use of aluminum alloy cubes to vary the ratio of transverse to axial strain and to Mr. Samuel Levy for the analysis given in appendix 1.

NOTATION

ϵ_a strain parallel to axis of wire strain gage

$\Delta\epsilon_a$ change in strain ϵ_a

ϵ_t strain transverse to axis of wire strain gage

$\Delta\epsilon_t$ change in strain ϵ_t

R resistance of gage, ohms

ΔR change in gage resistance, ohms

K_a axial sensitivity of gage = calibration factor for zero transverse strain, ohms per ohm per inch per inch.

K_t transverse sensitivity of gage = calibration factor for zero axial strain, ohms per ohm per inch per inch

μ Poisson's ratio

K_1 calibration factor of gage for uniaxial stress increment producing a strain $\Delta\epsilon_a$ parallel to the gage axis and a strain $-\mu\Delta\epsilon_a$ transverse to the gage axis, ohms per ohm per inch per inch.

K_2 calibration factor of gage for uniaxial stress increment producing a strain $\Delta\epsilon_t$ transverse to the gage axis and a strain $-\mu\Delta\epsilon_t$ parallel to the gage axis, ohms per ohm per inch per inch

APPARATUS AND METHOD

Description of Strain Gages

Six aircraft companies, the NACA Ames Aeronautical Laboratory, the Baldwin Locomotive Works, and the Chrysler Corporation contributed test gages of 15 different types (A, B, ..., G, H-1, I, ..., O), which in all but one case are identical with the gage types reported in reference 1. With the exception of gage type H-1, which was substituted by the maker for gage type H, table 1 of reference 1 gives a description of the test gages and figures 1 and 2 of reference 1 show the gages attached to strips used in the calibrations at low tensile strains. Data on gage type H-1 are given in appendix 1 of reference 2.

Calibrations

The output, $\Delta R/R$, of the gage was assumed to be a linear function of the strains acting along and transverse to the gage axis. This assumption is supported by the linearity of the experimental data, as explained in appendix 1.

The axial and transverse sensitivities K_a and K_t of the gages were related to gage output by

$$\frac{\Delta R}{R} = K_a(\Delta\epsilon_a) + K_t(\Delta\epsilon_t) \qquad (1)$$

and were calculated for each gage from measurements of unit change in gage resistance corresponding to known changes in strains ϵ_a and ϵ_t. These strains were applied

by placing the gage in a uniaxial stress field first with the axis of the gage parallel to the major principal strain and second with the axial transverse to the major principal strain. The positioning of the gages in the stress field was accomplished by attaching the gages to one pair of parallel faces of a dural cube that could be loaded in compression between either pair of parallel surfaces upon which no gages were attached. In this manner equation (1) could be written for two different ratios of $\Delta\epsilon_t$ to $\Delta\epsilon_a$, that is, $-\mu$ and $-1/\mu$.

The expressions for evaluating k_a and k_t were derived as follows. With gages attached to a 3.5-inch cube as shown at the left in figure 1, and with the cube uniformly loaded parallel to axis 1-1, equation (1) becomes,

$$\left(\frac{\Delta R}{R}\right)_1 = K_a(\Delta\epsilon_a) - \mu K_t(\Delta\epsilon_a) \tag{2}$$

since

$$\Delta\epsilon_t = -\mu(\Delta\epsilon_a) \tag{3}$$

Dividing equation (2) by $\Delta\epsilon_a$,

$$K_1 = \left(\frac{\Delta R}{R}\right)_1 \times \frac{1}{\Delta\epsilon_a} = K_a - \mu K_t \tag{4}$$

where K_1 is the calibration factor of a gage for a uniaxial stress increment producing a change in strain $\Delta\epsilon_a$ parallel to the gage axis and a change in strain $-\mu\Delta\epsilon_a$ transverse to the gage axis.

If the cube is now rotated 90° and loaded parallel to axis 2-2 as shown at the right in figure 1, equation (1) becomes,

$$\left(\frac{\Delta R}{R}\right)_2 = -\mu K_a(\Delta\epsilon_t) + K_t(\Delta\epsilon_t) \tag{5}$$

since

$$\Delta\epsilon_a = -\mu\Delta\epsilon_t \tag{6}$$

Dividing equation (5) by $\Delta\epsilon_t$

$$K_2 = \left(\frac{\Delta R}{R}\right)_2 \times \frac{1}{\Delta \epsilon_t} = K_t - \mu K_a \tag{7}$$

Solving equations (4) and (7) simultaneously for K_a and K_t,

$$K_a = \frac{K_1 + \mu K_2}{1-\mu^2} \tag{8}$$

$$K_t = \frac{K_2 + \mu K_1}{1-\mu^2} \tag{9}$$

Four values of K_1 and K_2 were calculated for each gage by substituting in equations (4) and (7) measured values of $(\Delta R/R)_1$ and $\Delta \epsilon_a$ obtained with the cube loaded parallel to axis 1–1, and $(\Delta R/R)_2$ and $\Delta \epsilon_t$ obtained with the cube loaded parallel to axis 2–2. Using the experimentally determined value of Poisson's ratio for the cube

$$\mu = 0.342 \tag{10}$$

values for K_a and K_t for each gage were calculated by substituting in equations (8) and (9) average values of K_1 and K_2 for each gage.

The unit changes in gage resistance $(\Delta R/R)_1$ and $(\Delta R/R)_2$ were measured as the major principal strain was increased from -1×10^{-4} to -15.7×10^{-4}.

Description of Cubes

Three cubes were used in the calibrations, and were placed one on top of another to form the column shown in figure 2. Wire gages were attached to the middle cube at the center portion of two faces. Each cube was machined from a 4-inch square bar of 24S-T aluminum alloy and ground to 3.500 inches between parallel surfaces. The four load bearing surfaces of the center cube and the adjoining surfaces of the end cube were lapped to obtain optical surfaces, flat within about 0.00002 inch.

Poisson's ratio for the cube and the strain distribution on the two surfaces upon which wire strain gages were to be attached were determined with Tuckerman strain gages with the cube in each of its two loading positions. The strain surveys indicated linear variations in axial strain across

the face of the column at the midsection which did not exceed 3 percent. Variations in transverse strain between the upper and lower edges of the center cube did not exceed 0.5 percent. During calibrations errors due to nonuniform strain distribution were minimized by calibrating the wire gages individually and measuring local strains with Tuckerman gages spanning the wire strain gages. The four load bearing surfaces of the cube were chosen parallel to the axis of the bar from which the cube was cut so that the cube was always loaded transverse to the direction of rolling. The average axial strain and the average transverse strain over the face of the cube were measured with 2-inch Tuckerman strain gages for the strain inverval used in the calibrations. The ratios of average transverse to average axial strains were

$$-0.341, \quad -0.344$$

for the two directions of loading, respectively. The ratios for strains measured with 2-inch Tuckerman strain gages in the center portion of the faces to which the wire strain gages were attached ranged from −0.334 to −0.347 and averaged,

$$-0.342$$

This average value was assumed to hold for both loading positions of the cube and was used in all wire gage calculations.

Strain and Resistance Measurements

The calibrating strain applied to each wire gage was measured with a Tuckerman optical strain gage. The unit change in resistance of each gage during calibration was measured with a Wenner-type ratio set in a direct-current Wheatstone bridge, using a high-sensitivity moving-coil galvanometer as a null indicator. The construction of the ratio set and its use in the bridge circuit to measure unit change in resistance has been described in reference 1. The voltage drop across the gage during calibration was 0.75 volt when the axis of the gage was parallel to the major principal strain, and 1.5 volt when the axis of the gage was transverse to the major principal strain. The higher voltage in the latter case served only to increase the bridge sensitivity for the measurement of the decreased gage output under transverse loading.

TEST PROCEDURE

Attachment of Gages

Four gages of each type were calibrated. All gages were attached at the National Bureau of Standards following the makers instructions. Gages were attached with bonding cements supplied by the maker and were dried a total of 42 hours as follows: 18 hours at room temperature following attachment, 7 hours with the cube heated by radiation from a 60-watt lamp to about 120° F, and 17 hours additional at room temperature. No gages were waterproofed.

Tests

Two gages of a given type were attached to each of two parallel gage surfaces of the test cube, which was then loaded in compression in the position shown at the left in figure 1. The laboratory setup for the tests is shown in figure 2. A Tuckerman strain gage was mounted on the cube along axis A–A (fig. 1) so as to span one of the four gages and indicate the strain ϵ_a applied to this gage. The wire gage spanned by the Tuckerman gage was connected in one arm of a Wheatstone bridge which measured the unit change in gage resistance $(\Delta R/R)_1$ resulting from a change in the applied ϵ_a. The cube was first preloaded to 190,000 pounds ($\epsilon_\epsilon = -15.7 \times 10^{-4}$) for three cycles of loading to reduce zero shift in the gages (reference 1). Loads of 10,000, 190,000, and 10,000 pounds were then applied in succession. At each load the Tuckerman gage was read at the instant of balance of the Wheatstone bridge. The loading cycle was then repeated for an additional set of Tuckerman gage and bridge readings. From these measurements four values of K_1, equation (4), were calculated for this gage: two for increasing strain and two for decreasing strain. The remaining gages on the cube were individually calibrated for K_1 values in the same manner. The Tuckerman gage was moved from one wire gage to another and individual gages were connected in the Wheatstone bridge in turn.

Temperature compensating gages were not used in the calibrations since the loading cycles, during which measurements were made, required less than 3 minutes, and the mass of the column was large enough to be insensitive to small variations in ambient temperature in this interval of time.

Following the measurements of $(\Delta R/R)_1$ and $\Delta\epsilon_a$ on each of the four gages, the cube was rotated 90^0 and loaded as shown at the right in figure 1. The laboratory setup for the tests is shown in figure 3. The Tuckerman gage was mounted on the cube along axis B-B (fig. 1) so as to span both wire gages on this surface of the cube and indicate the strain ϵ_t applied to the gages. One of the gages was connected in the Wheatsone bridge which measured the unit change in resistance $(\Delta R/R)_2$ resulting from a change in the strain ϵ_t applied to this gage. After three preloading cycles, the cube was subjected to the same loading cycles as before, and at each load the Tuckerman gage was read at the instant of bridge balance. From these measurements four values of K_2, equation (7), were calculated for this gage: two for increasing strain and two for decreasing strain. The remaining gages on the cube were individually calibrated for K_2 values in the same manner.

The axial sensitivity K_a and the transverse sensitivity K_t were then calculated for each of the four gages of this type by substituting in equations (8) and (9) the average of the four values of K_1 and the average of the four values of K_2 obtained for each gage.

RESULTS AND DISCUSSION

The axial and transverse sensitivities K_a and K_t as defined by equation (1) are given in table 1 together with the ratio K_t/K_a for each gage. The gage types are arranged in table 2 in the order of increasing values of the average ratio K_t/K_a, for each gage type.

The average ratio K_t/K_a, which is a measure of the response of a gage to transverse strain relative to its response to axial strain, ranged from −0.063 for gages of type G to +0.028 for gages of type F. The average ratios K_t/K_a were positive and did not exceed 0.028 for 11 of the 15 types of gages. Negative ratios ranging from −0.007 to −0.063 were found for four types of gages (G, L, M, and N). Table 2 shows that the average ratio K_t/K_a for gages H-1, J, A, C, and O were less than 0.003, so that for gages of these types the response to transverse strain was less than 0.3 percent of the response to axial strain.

The average ratios K_t/K_a measured for the different gages are compared with theoretical ratios based on the geometry of the gage windings in figure 4.

The theoretical ratio of the transverse sensitivity to the axial sensitivity (γ) was taken as the ratio of the effective length of transverse wire to the effective length of longitudinal wire in each winding. The strain-sensitive wire grids for all but one of the gages (M) could be represented by two general grids shown in figure 4, a parallel strand winding and a saw-toothed winding, which could be divided into nominally straight wires and semicircular loops. For purposes of analysis the transverse sensitivity of each gage was assumed to be due entirely to the semicircular loops at the ends of adjacent wire strands. Slanting of the longitudinal wires in the saw-toothed grids (gages A and C only) was ignored since, for small angles between these wires and the axis of the gage, the slanting contributes negligible transverse effect compared to the loops at the ends of adjacent strands. Since the sum of the strains in any two perpendicular directions is constant, the average circumferential strain in the semicircular loop may be obtained by splitting the loop into two quadrants of a circle, one subjected to a constant circumferential strain ϵ_a and the other to a constant circumferential strain ϵ_t. The effective length of transverse wire W_t is therefore equal to half the sum of the semicircular arc lengths in the grid,

$$W_t = \frac{\pi d}{4}(n-1) \tag{11}$$

The effective length of longitudinal wire W_a is equal to the sum of the straight wire lengths ($ng+2a$) plus the sum of the remaining halves of the semicircular loops. The theoretical ratio of transverse sensitivity to axial sensitivity is

$$\gamma = \frac{\frac{\pi d}{4}(n-1)}{ng + \frac{\pi d}{4}(n-1) + 2a} \tag{12}$$

Figure 4 shows that with the exception of the points involving negative values of K_t/K_a (gages G, L, and N) the points scatter about a faired curve through the origin. The scatter is large, however, possibly due to differences in the type of base paper, bonding cement, and strain-sensitive wire used in the different gages in addition to inaccuracies in the measurements of K_t/K_a and (γ). Examination of figure 4 also shows that the points lie below the line of unit slope (dotted) so that the measured ratios K_t/K_a were all less

than the theoretical ratio (γ). This was ascribed to a decrease in the efficiency with which the bonding cement transfers strain to wire in loops of small diameter. The dotted points in figure 4 include a correction for transverse sensitivity of the wire for gages L and N. This correction will be discussed below.

Gage M, which also had a negative ratio K_t/K_a, is not included in figure 4 since the expression for γ is not applicable to the winding in this gage. Gage M has a double layer of wires parallel to the surface of the gage, and the loops between adjacent upper and lower strands are in planes perpendicular to the surface of the gage; hence γ as defined in equation (12) cannot apply. In all gages except M the strain-sensitive wire was confined to a single plane.

The negative transverse sensitivities found for gages of type M were believed to be due to the geometry of the strain-sensitive winding. The upper and lower layers of wire, separated by bonding cement and a thickness of paper, form a small structure which contracts in the direction normal to the surface of the gage when the gage is subjected to a transverse tensile strain and zero axial strain. The contraction produces a compressive strain in the loops of wire between the ends of the upper and lower strands, which, in turn, decreases the resistance of the wire in these sections and leads to negative transverse sensitivity K_t (equation (1)). The transverse sensitivity of a gage with this type of winding ("wrap-around") may be negative, however, only so long as the unit change in gage resistance due to the afore-mentioned action of the loops exceeds the unit change in gage resistance due to the positive effect of the transverse projections of the longitudinal wires which result from spacing successive turns. The transverse sensitivity of a gage of type M was actually changed from a negative to a positive value by removing one gage length of the outside wire strand from its usual position and rewinding this length transverse to the gage axis. This effect may be utilized for winding gages similar to type M which are insensitive to transverse strain, provided it is possible to wind them in a sufficiently uniform manner.

The negative transverse sensitivities found for gages of types G, L, and N were surprising since these gages all have parallel strand grids (sketch at left in fig. 4) with relatively large loops, which should presumably produce positive transverse sensitivities. These three gage types differed from other gages primarily in the type of strain-

sensitive wire used in the grid windings. Chromel, Chromel "C", and iso-elastic wires were used in gages G, L, and N; whereas all other gages were wound with advance wire or with wires having strain sensitivities near that of advance.

On the basis of the strain survey made on the cube, and with the known accuracies of the Tuckerman gage and the Wenner ratio set, it was estimated that the calibration factors K_1 and K_2 in equations (4) and (7) were each accurate within ±0.5 percent, and that Poisson's ratio of the cube was known within 1 percent. The values of K_a and K_t in table 1 were therefore estimated to be correct within $\Delta K_{a,t} = \pm 0.01$, and the ratio K_t/K_a correct within $\Delta(K_t/K_a) = \pm 0.005$. The average ratios K_t/K_a found for gages G, L, and N were −0.063, −0.007, and −0.027, respectively, which differ from zero by more than the estimated maximum error of ±0.005.

Additional calibrations were made on gages of types L and N, and were attempted on gages of type G, to check the reproducibility of results. In the case of gage G it was doubted that the average ratio K_t/K_a of −0.063 was representative of the gage in view of the large variation in the ratios for the individual gages of this type (−0.009 to −0.142, table 1). The average ratio −0.063 could not be checked because of erratic changes in the resistances of the gages on which additional calibrations were attempted. The average ratios found for four additional gages each of types L and N were −0.008 and −0.027 (table 1), which agree almost exactly with the values −0.007 and −0.027 given in table 2 for these gages.

Calibrations were then made on single strand gages (fig. 5) made up of strain-sensitive wire removed from gages of types G, L, and N and on single strand gages using new advance wire. The advance wire was included as representative of all gages which showed positive values of K_t. The results of these calibrations are given in table 3. The average ratio K_t/K_a for the advance wire was +0.001; whereas the average ratios for the single wires from gages G, L, and N were −0.022, −0.017, and −0.040, respectively. The ratios for wires G, L, and N were observed to be not only negative but two of them, L and N, were of larger magnitude than the K_t/K_a ratios found for the types of gages from which the wires were removed. Also the single wires from gages of type G showed only small variations in K_a, K_t, and K_t/K_a, indicating that the large variations

encountered with gages G were probably due to gage construction. The results of the calibrations on single wires suggested that the geometry of the grid windings in gages L and N actually produced a positive transverse sensitivity K_t which was obscured by a negative transverse sensitivity of the wire. The last column in table 3 gives the difference between the average ratio K_t/K_a for the complete gage and the average ratio for the single wire. This difference was taken as the ratio due to the geometry of the gage windings and was plotted as a dotted point in figure 4. Examination of figure 4 shows that the dotted points for gages L and N fit the curve considerably better than the solid points involving the true ratios.

The transverse sensitivities and the ratios of transverse to axial sensitivities for single wires of iso-elastic, chromel, advance, and manganin are plotted against the axial sensitivity in figure 6. A smooth curve could be plotted for the wires with axial sensitivities exceeding 2; the point for the manganin wire with an axial sensitivity of only 1 was far removed from this curve.

The pronounced negative transverse strain sensitivity wires with axial sensitivities well above 2 is an interesting experimental phenomenon which should be investigated further in order to explain the fundamental nature of strain sensitivity of fine wires.

Attention should be called to the possibility of utilizing the negative transverse sensitivity of wires such as iso-elastic or chromel for winding multistrand gages which are insensitive to transverse strain by making the loops between adjacent wire strands in these gages of such diameter as to compensate for the negative transverse sensitivity of the wire.

At the present time the writer has no explanation for the negative transverse sensitivities found for iso-elastic, chromel, and manganin wires when attached to structures under combined strain. Among the variables which might in some manner produce the negative values of the transverse sensitivity, K_t, may be considered:

1. Variations in gage current

2. Lack of temperature compensation

3. Differences in bonding

4. Resistance changes due to thermal effects accompanying deformation of the gage wires

Check calibrations were made on gage N with different bridge voltages (i.e., gage currents) with and without temperature compensation. The values of K_a and K_t obtained showed no significant change with voltage (0.75 to 1.5 volts) and were the same with and without temperature compensation.

The procedures for bonding the different wires in the tests of the single strand gages were identical; hence the various sensitivities appear to be a property of the wires rather than of the bond.

A computation on the assumption that all the strain energy in the gage wires is converted into heat indicates a temperature rise of the order of 0.1° F for a strain of 0.0015. The energy actually available for conversion into heat is only a small fraction of the strain energy and hence would produce a negligible change in temperature.

CONCLUSIONS

Calibrations on the 15 types of gages included in the program showed average ratios of transverse sensitivity K_t to axial sensitivity K_a which were positive and did not exceed $K_t/K_a = 0.028$ for 11 types of gages. The average ratio K_t/K_a did not exceed 0.002 for gages A, C, H-1, J, and O in this group.

The average ratio K_t/K_a was found to be negative for four types of gages (G, L, M, and N). The negative transverse sensitivity of gage M was ascribed to the geometry of the gage structure and grid winding. Calibrations on single strand gages constructed with strain-sensitive removed from gages of types G, L, and N showed that the negative transverse sensitivities of gages G, L, and N were due to characteristic negative transverse sensitivities of the wires. These gages were wound with chromel, chromel "C", and iso-elastic wires which had relatively high axial strain sensitivities (2.4 to 3.4); whereas all other gages were wound with advance wire, or wire having a strain sensitivity near that of advance (2.1), which showed no significant transverse sensitivity.

The presence of negative transverse sensitivity in single strand gages deserves further study to explain the fundamental nature of strain sensitivity in the fine wires.

It is suggested that the negative transverse sensitivity characteristic of certain types of wire may be utilized to wind multistrand gages with zero transverse sensitivity; in these gages the negative transverse sensitivity of the wire would be compensated by introducing an equal amount of positive transverse sensitivity with end loops of the proper diameter.

National Bureau of Standards,
Washington, D. C. October 31, 1945.

REFERENCES

1. Campbell, William R.: Performance Tests of Wire Strain Gages. I – Calibration Factors in Tension. NACA TN No. 954, 1944.

2. Campbell, William R.: Performance Tests of Wire Strain Gages. II – Calibration Factors in Compression. NACA TN No. 978, 1945.

3. Campbell, William R.: Performance Tests of Wire Strain Gages. III – Calibrations at High Tensile Strains. NACA TN No. 997, 1945.

APPENDIX 1

Derivation of Equation (1) from Linearity of Experimental Data

Assume to begin with that the output of the gage is some analytical function of the axial and transverse strains. Expanding this function in the form of a Taylor series gives:

$$\frac{\Delta R}{R} = A\epsilon_a + B\epsilon_t + C\epsilon_a^2 + D\epsilon_a \epsilon_t + E\epsilon_t^2 + \ldots \qquad (13)$$

The strains ϵ_a and ϵ_t in the present calibrations are related for the two directions of loading on the cube by

$$\left.\begin{aligned} 1.\ \epsilon_t &= -\mu\epsilon_a \\ 2.\ \epsilon_t &= -\frac{1}{\mu}\epsilon_a \end{aligned}\right\} (14)$$

and equation (13) may be written

$$\left.\begin{aligned} \left(\frac{\Delta R}{R}\right)_1 &= \epsilon_a(A - B\mu + C\epsilon_a - D\mu\epsilon_a + E\mu^2\epsilon_a + \ldots \\ \left(\frac{\Delta R}{R}\right)_2 &= \epsilon_t(-A\mu + B + C\mu^2\epsilon_t - D\mu\epsilon_t + E\epsilon_t + \ldots \end{aligned}\right\} (15)$$

or

$$\left.\begin{aligned} \left(\frac{\Delta R}{R}\right)_1 &= \epsilon_a (A - \mu B) + \epsilon_a^2(C - \mu D + \mu^2 E) + \ldots \\ \left(\frac{\Delta R}{R}\right)_2 &= \epsilon_t (-\mu A + B) + \epsilon_t^2(\mu^2 C - \mu D + E) + \ldots \end{aligned}\right\} (16)$$

Since it is known that to a high degree $(\Delta R/R)_1$ and $(\Delta R/R)_2$ are linear with ϵ_a and ϵ_t, respectively, for the two testing conditions, it follows that the coefficients of the nonlinear terms in equation (16) must be equal to zero:

$$\left.\begin{aligned} C - \mu D + \mu^2 E &= 0 \\ \mu^2 C - \mu D + E &= 0 \end{aligned}\right\} \quad (17)$$

It is mathematically possible to satisfy these equations by values of C, D, E, ... which are different from zero. However, this leads to an improbable type of function (13). It is far more probable that (17) is satisfied by having all nonlinear coefficients in (13) equal to zero:

$$C = D = E = \ldots = 0 \quad (18)$$

A definite proof of equation (18) would require calibrations under combined strain such that the ratio ϵ_a/ϵ_t is variable over a wide range.

TABLE 1.- RESULTS OF CALIBRATIONS

Gage type	Gage No.	Resistance, R (ohms)	K_1 (equation (4))	K_2 (equation (7))	K_a	K_t	K_t/K_a	Average K_t/K_a
A	1	118.2	2.008	-0.685	2.008	0.002	0.001	
	2	118.1	2.044	-.694	2.046	.006	.003	
	3	114.7	2.067	-.707	2.068	.001	.000	
	4	114.2	2.079	-.705	2.081	.006	.003	0.002
B	1	99.7	2.146	-.724	2.150	.011	.005	
	2	99.9	2.134	-.719	2.138	.012	.006	
	3	99.9	2.123	-.709	2.130	.021	.010	
	4	99.7	2.118	-.712	2.123	.014	.007	-.007
B*	5	99.9	2.119	-.714	2.123	.012	.006	
	6	99.8	2.127	-.713	2.133	.016	.008	
	7	99.7	2.191	-.750	2.191	.001	.000	
	8	99.8	2.109	-.707	2.115	.016	.008	.006
C	1	90.0	2.050	-.701	2.050	.000	.000	
	2	91.0	2.045	-.692	2.048	.008	.004	
	3	87.3	2.042	-.695	2.043	.004	.002	
	4	89.9	2.044	-.693	2.046	.007	.003	.002
D	1	119.9	2.069	-.683	2.079	.028	.013	
	2	119.3	2.069	-.682	2.079	.029	.014	
	3	119.4	2.070	-.683	2.080	.028	.013	
	4	119.4	2.078	-.681	2.090	.034	.016	.014
E	1	399.5	2.158	-.716	2.167	.025	.012	
	2	398.9	2.110	-.701	2.118	.023	.011	
	3	399.3	2.121	-.708	2.128	.020	.009	
	4	399.7	2.144	-.712	2.152	.024	.011	.011
F	1	119.9	2.019	-.638	2.039	.060	.029	
	2	119.8	2.018	-.641	2.037	.056	.027	
	3	119.9	2.025	-.641	2.045	.059	.029	
	4	120.0	2.024	-.640	2.044	.059	.029	.028
G	1	120.6	2.263	-.792	2.256	-.020	-.009	
	2	120.1	2.320	-.911	2.275	-.133	-.058	
	3	120.3	2.092	-.793	2.062	-.088	-.043	
	4	120.8	1.882	-.869	1.795	-.255	-.142	-.063
H-1	1	119.9	2.058	-.699	2.060	.005	.002	
	2	120.2	2.035	-.695	2.035	.001	.000	
	3	120.2	2.013	-.688	2.013	.000	.000	
	4	120.1	2.038	-.690	2.041	.007	.003	.001
I	1	120.2	2.139	-.722	2.143	.011	.005	
	2	120.0	2.145	-.717	2.152	.019	.009	
	3	119.0	2.150	-.718	2.156	.019	.009	
	4	120.2	2.155	-.719	2.162	.024	.011	.008

* Four additional gages calibrated to check for reproducibility of results.

TABLE 1.-(Continued)

Gage type	Gage No.	Resistance, R (ohms)	K_1 (equation (4))	K_2 (equation (7))	K_a	K_t	K_t/K_a	Average K_t/K_a
J	1	300.0	2.094	-0.713	2.095	0.004	0.002	
	2	299.8	2.091	-.713	2.092	.002	.001	
	3	300.0	2.090	-.713	2.091	.003	.001	
	4	300.2	2.068	-.708	2.068	.000	.000	0.001
K	1	50.1	2.152	-.718	2.160	.022	.010	
	2	50.1	2.192	-.723	2.203	.031	.014	
	3	50.0	2.132	-.708	2.140	.025	.012	
	4	50.1	2.145	-.710	2.154	.027	.013	.012
L	1	120.7	2.323	-.806	2.318	-.013	-.006	
	2	118.6	2.316	-.811	2.309	-.022	-.010	
	3	119.6	2.272	-.791	2.267	-.016	-.007	
	4	119.6	2.316	-.820	2.311	-.013	-.006	-.007
L*	5	118.6	2.244	-.778	2.240	-.012	-.005	
	6	119.9	2.286	-.805	2.277	-.026	-.011	
	7	118.1	2.294	-.802	2.287	-.020	-.009	
	8	118.2	2.283	-.797	2.277	-.018	-.008	-.008
M	1	119.1	1.941	-.680	1.934	-.019	-.010	
	2	118.4	1.934	-.672	1.930	-.012	-.006	
	3	119.0	1.948	-.678	1.944	-.013	-.007	
	4	119.1	1.980	-.683	1.978	-.007	-.004	-.007
M*	5	120.2	1,976	-.685	1.973	-.010	-.005	
	6	119.8	1.933	-.669	1.930	-.009	-.005	
	7	120.3	1.932	-.674	1.927	-.015	-.008	
	8	120.2	1.963	-.677	1.961	-.006	-.003	-.005
N	1	501.9	3.435	-1.247	3.408	-.082	-.024	
	2	500.9	3.437	-1.252	3.408	-.086	-.025	
	3	501.5	3.368	-1.245	3.333	-.105	-.032	
	4	500.1	3.337	-1.238	3.357	-.090	-.027	-.027
N*	5	501.7	3.401	-1.255	3.366	-.104	-.031	
	6	501.3	3.437	-1.250	3.409	-.084	-.025	
	7	502.9	3.443	-1.256	3.413	-.089	-.026	
	8	500.8	3.397	-1.244	3.366	-.093	-.027	-.027
O	1	100.1	2.096	-.712	2.098	.005	.002	
	2	100.4	2.103	-.713	2.105	.007	.003	
	3	100.2	2.098	-.712	2.100	.006	.003	
	4	99.9	2.083	-.710	2.084	.003	.001	.002

* Four additional gages calibrated to check for reproducibility of results.

TABLE 2.- SEQUENCE OF GAGES IN ORDER OF INCREASING VALUES OF AVERAGE RATIO K_t/K_a

Gage type	Average[1] K_t/K_a
G	−0.063
N	−.027
M	−.007
L	−.007
H−1	.001
J	.001
A	.002
C	.002
O	.002
B	.006
I	.008
E	.011
K	.012
D	.014
F	.028

[1]From table 1.

TABLE 3.- RESULTS OF CALIBRATIONS ON SINGLE STRAND GAGES[1]

Wire removed from gages of type	Wire alloy	Gage No.	Resistance (ohms)	$(K_a)_w$	$(K_t)_w$	$\left(\frac{K_t}{K_a}\right)_w$	Averages $\left(\frac{K_t}{K_a}\right)_w$	Averages $\left(\frac{K_t}{K_a}\right)_g$	Difference of averages $\left(\frac{K_t}{K_a}\right)_g - \left(\frac{K_t}{K_a}\right)_w$
G	Chromel (0.002 in.)	1	20.4	2.542	-0.054	-0.021	-0.022	--	-0.041
		2	20.5	2.556	-.060	-.023			
		3	20.2	2.561	-.057	-.023			
		4	20.5	2.561	-.052	-.020			
L	Chromel C (0.005 in.)	1	92.4	2.433	-.045	-.018	-.017	-0.007	+.010
		2	93.7	2.414	-.046	-.019			
		3	91.2	2.412	-.040	-.017			
		4	93.9	2.402	-.042	-.017			
		5	91.0	2.443	-.042	-.017			
N	Iso-elastic (0.005 in.)	1	120.2	3.496	-.138	-.038	-.040	-.027	+.013
		2	121.3	3.509	-.140	-.040			
		3	122.5	3.415	-.141	-.041			
		4	118.0	3.441	-.137	-.040			
-	Advance (0.001 in.)	1	42.5	2.139	-.004	-.002	+.001	---	---
		2	45.3	2.133	-.001	-.000			
		3	41.4	2.145	+.004	+.002			
		4	42.5	2.143	+.005	+.003			
		5	44.8	2.148	+.007	+.003			
		6	42.2	2.146	+.002	+.001			
-	Manganin (0.001 in.)	1	44.3	.983	-.014	-.014	-.012	--	---
		2	44.1	.984	-.012	-.012			
		3	44.0	.982	-.011	-.011			
		4	45.4	.992	-.013	-.013			

[1]Subscript w denotes value for single strand gage. Subscript g denotes value for complete gage of type from which wire was removed to construct single strand gage.

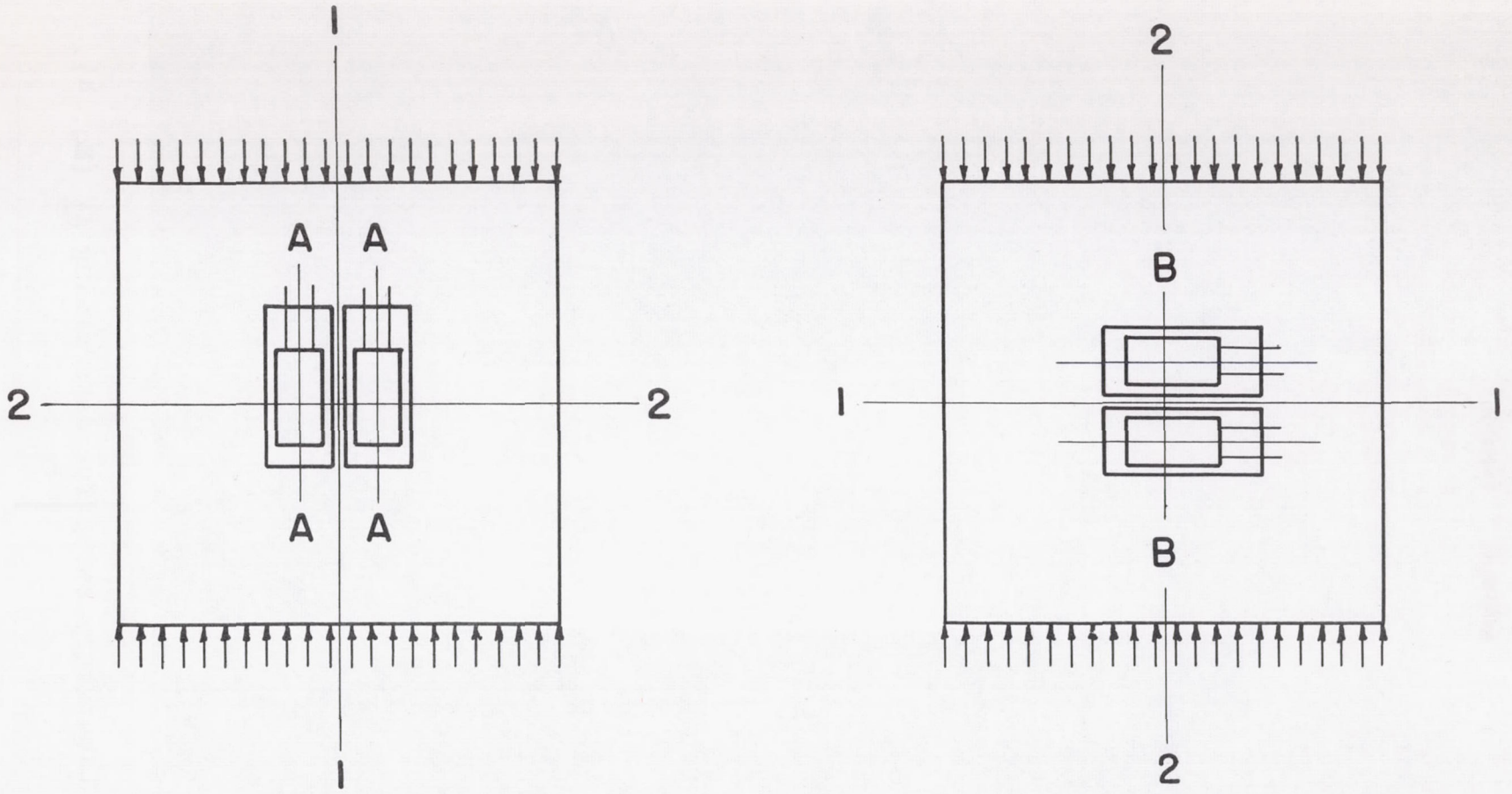

Figure 1.- Test cube, showing location of wire strain gages and loading positions of cube during calibrations. Two wire strain gages were also attached to the surface opposite the surface shown. Tuckerman strain gage locations during calibration are indicated by A-A and B-B.

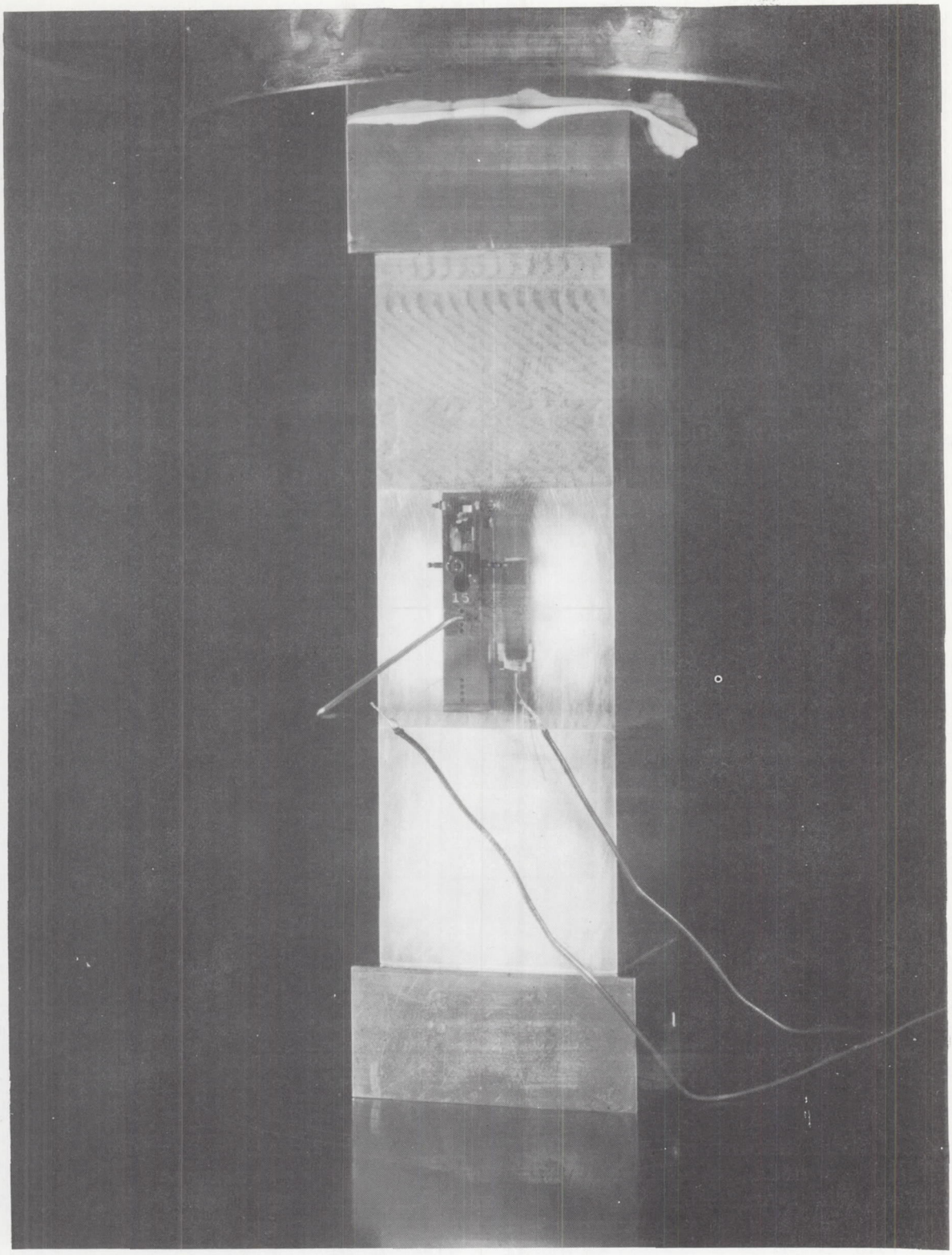

Figure 2.- Laboratory setup for determining K_1 (Eq. 4).

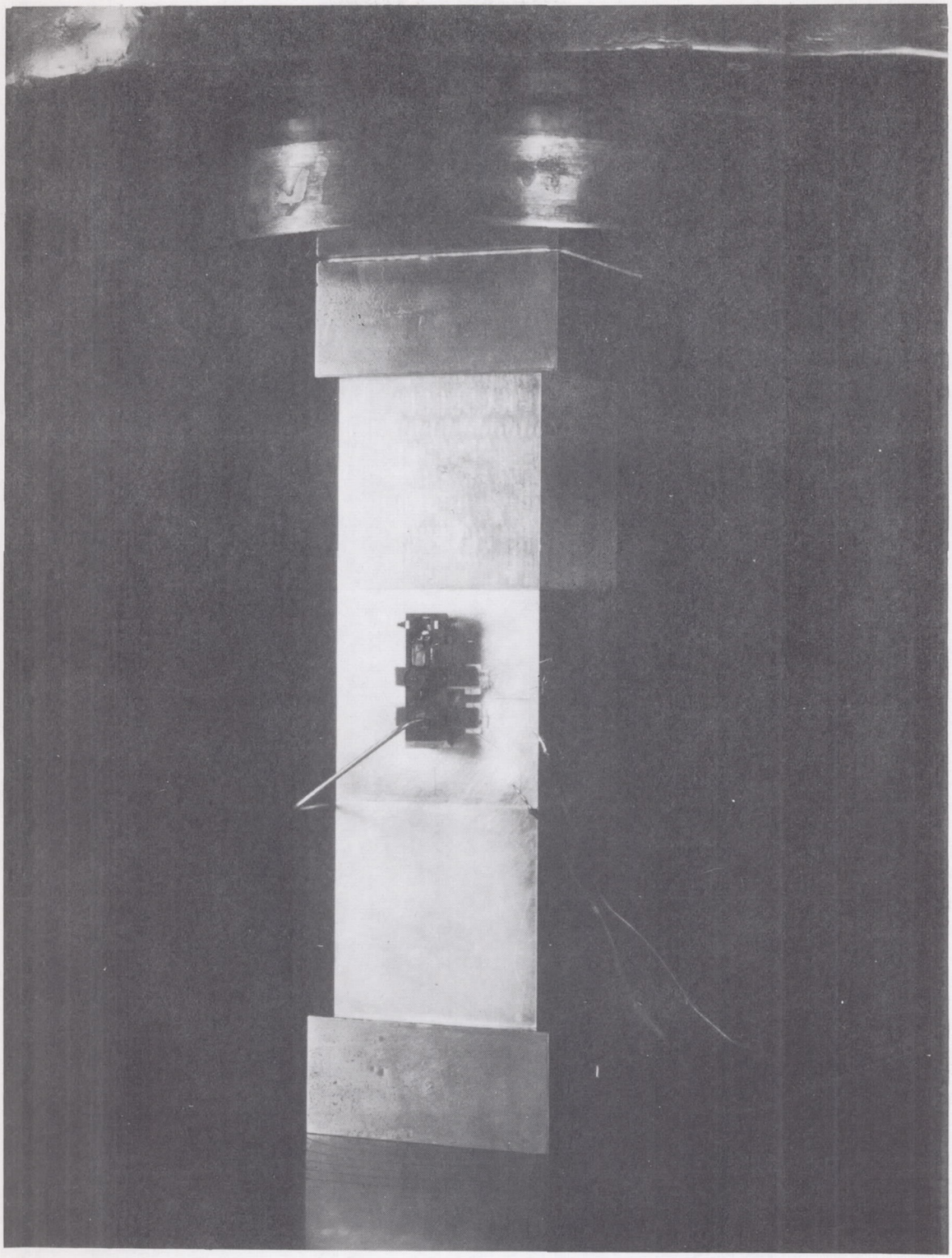

Figure 3.- Laboratory setup for determining K_2 (Eq. 7).

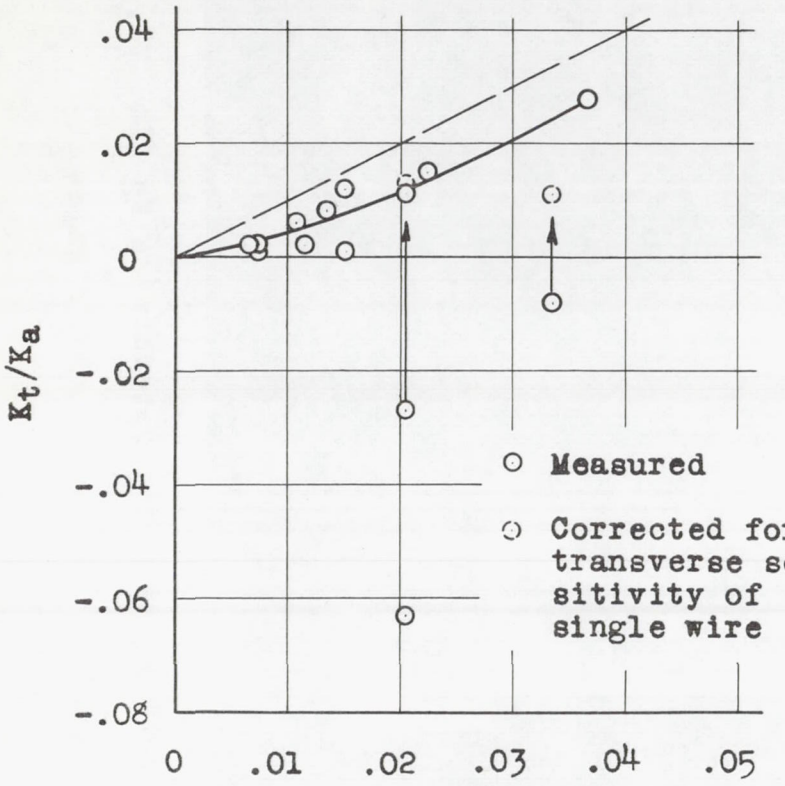

$$\gamma = \frac{\frac{\pi d}{4}(n-1)}{ng + \frac{\pi d}{4}(n-1) + 2a}$$

Gage type	$\frac{K_t}{K_a}$ *	γ **	Gage type	$\frac{K_t}{K_a}$	γ
A	.002	.0064	H-1	.001	.0152
B	.006	.0108	I	.008	.0134
C	.002	.0114	J	.001	.0074
D	.015	.0224	K	.012	.0150
E	.011	.0206	L	-.008	.0337
F	.028	.0366	N	-.027	.0205
G	-.063	.0206	O	.002	.0072

* Average values (from table 2).

** $\gamma = \dfrac{\frac{\pi d}{4}(n-1)}{ng + \frac{\pi d}{4}(n-1) + 2a}$ (See sketches below)

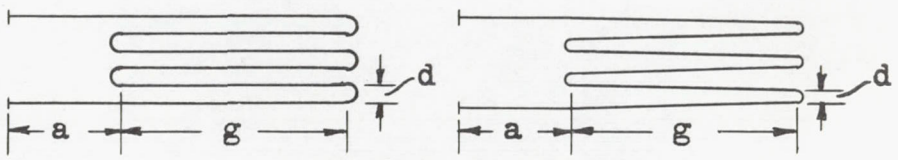

n = number of strands

Figure 4.- Comparison of theoretical and experimental values of the ratio K_t/K_a.

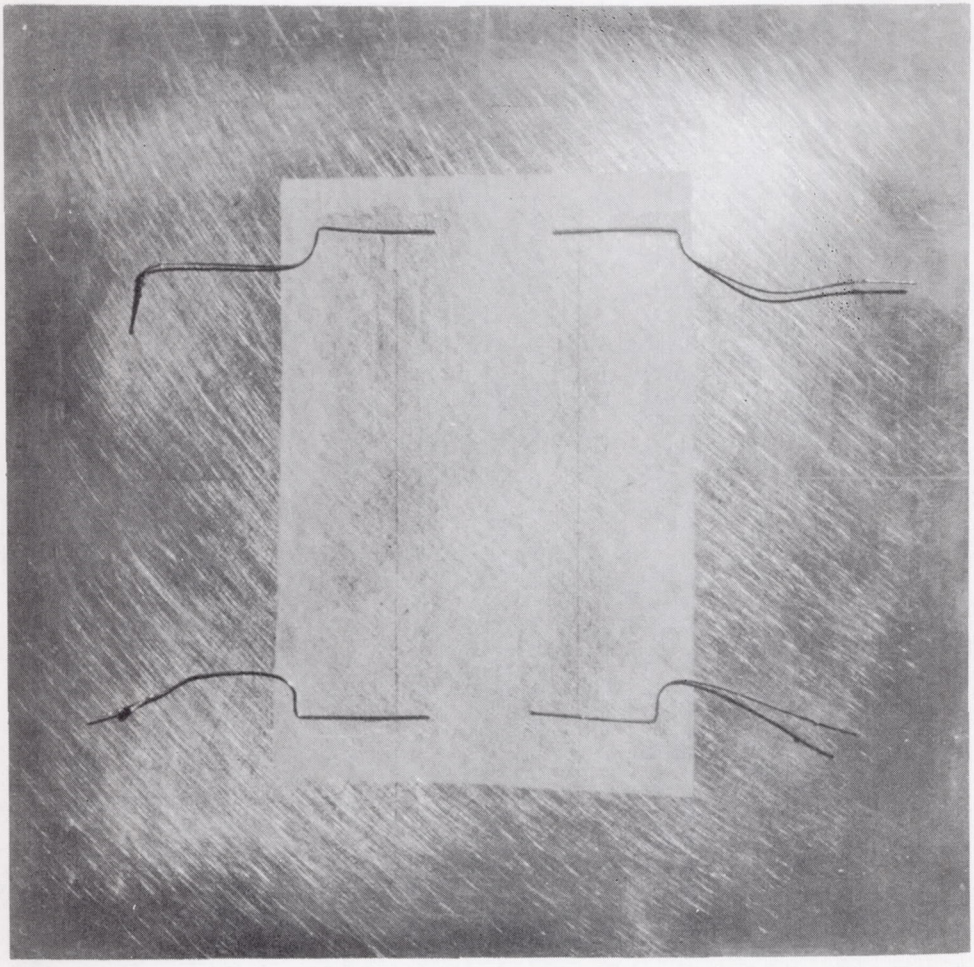

Figure 5.- Single strand wire strain gages.

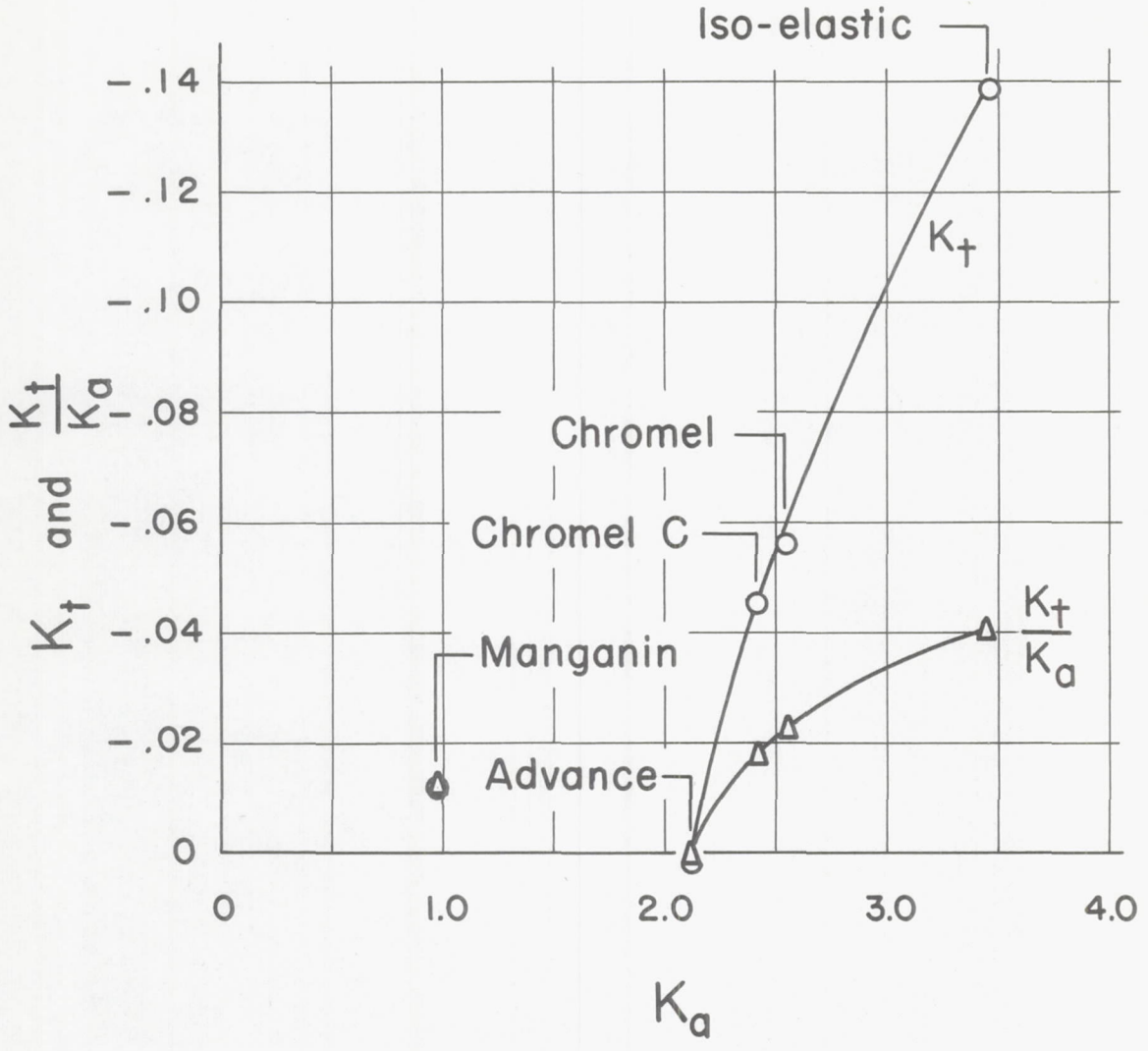

Figure 6.- Curves of K_t/K_a and K_t vs. K_a for different types of strain-sensitive wire.

NACA-Langley - 5-10-54 - 125